THE SOCIETY AND COLLEGE OF RADIOGRAPHERS

Pulse sequences for contrast-enhanced magnetic resonance imaging

Martin J. Graves*

Departments of Radiology and Medical Physics, Cambridge University Hospitals NHS Foundation Trust, Cambridge, CB2 2QQ, UK

Abstract   The theory and application of magnetic resonance imaging (MRI) pulse sequences following the administration of an exogenous contrast agent are discussed. Pulse sequences are categorised according to the contrast agent mechanism: changes in proton density, relaxivity, magnetic susceptibility and resonant frequency shift. Applications in morphological imaging, magnetic resonance angiography, dynamic imaging and cell labelling are described. The importance of optimising the pulse sequence for each application is emphasised.
© 2006 The College of Radiographers. Published by Elsevier Ltd. All rights reserved.

Introduction

Contrast agents have been used in NMR since the earliest days when Bloch added paramagnetic ferric ions in solution to shorten the longitudinal relaxation time (T_1) of protons in water.[1] Development of the first commercially available contrast agent for MRI was started around 1981[2] with the first reported use in humans in 1984.[3] Since then the range and applicability of contrast agents have grown tremendously, in many cases driving the development of MRI pulse sequences to exploit the behaviour of the contrast agent. This article will review some of the main pulse sequences for contrast-enhanced MRI. It is beyond the scope of this article to describe the principles of MRI sequences in detail,

for further information the reader is referred to one of the standard MRI textbooks.[4]

It should be noted that unlike the exogenous contrast material used in X-ray investigations MRI does not generally directly visualise the contrast material itself but rather observes the indirect ''effect'', that the material has on the local water proton signal, usually via relaxivity or susceptibility mechanisms. Consequently contrast material in MRI is often referred to as a contrast ''agent'' in contradistinction to the contrast ''media'' that is directly visualised in X-ray investigations.

The discussion of pulse sequences will be divided into the four ways in which exogenous contrast materials can be considered to act:

1. *Proton density.* Increasing or decreasing the numbers of protons within a tissue compartment can modify the proton density within a voxel.

* Tel.: +44 01233 336897; fax: +44 01233 220915.
E-mail address: mjg40@radiol.cam.ac.uk

2. *Relaxation times.* The T_1 and T_2 relaxation times of tissues can be reduced by the administration of an extracellular paramagnetic agent such as a chelate of the metal ion gadolinium (Gd^{3+}), or by the use of an intracellular agent such as superparamagnetic iron oxide (SPIO) particles.

3. *Magnetic susceptibility.* Contrast agents with a large magnetic moment such as Gd^{3+} can reduce the local magnetic field homogeneity.

4. *Resonant frequency shift.* The resonant MRI frequency can be shifted by the use of agents that have negligible nuclear relaxation properties but large electron-spin relaxation characteristics such as dysprosium Dy^{3+} or SPIO particles.

Proton density

In certain body areas, e.g. the gastrointestinal (GI) tract, it is possible to artificially change the proton density thereby improving the luminal contrast. For example, CO_2 may be used as a negative contrast agent for the stomach, small bowel or colon by reducing the proton density.[5] Conversely it is possible to obtain a positive contrast, by increasing the proton density, using oral water alone[6] or with polyethylene glycol (PEG),[7] or to perform MR enteroclysis using water with methyl cellulose.[8] These examples are slightly exceptional in our discussion of exogenous contrast material because we are using them primarily as a contrast media rather than as an agent.

The signal intensity observed from any standard MRI pulse sequence has a dependency on the proton density (ρ). Eq. 1 is a simplified expression that describes the signal intensity (SI) for a spin echo imaging sequence in which the repetition time (TR) is much longer than the echo time (TE).

$$SI \propto \rho \left[1 - e^{-\frac{TR}{T_1}} \right] e^{-\frac{TE}{T_2}} \tag{1}$$

In order to maximise the contrast between any two tissues based on the proton density it would therefore be necessary to minimise the effects of T_1 relaxation by making the TR as long as possible and minimising the effects of T_2 by making the TE as short as possible.

Since imaging the GI tract generally requires fast imaging in order to minimise artefacts from motion, e.g. peristalsis, coherent gradient echo or fast spin echo (FSE) imaging techniques are often employed.[9] In an FSE sequence multiple echoes, known as the echo train length (ETL), are acquired per TR. This has the advantage of reducing the overall acquisition time by a factor given by the ETL. The echo train acquired during each TR is often referred to as a shot. It is possible to acquire all echoes in a single TR period, this is known as single shot fast spin echo (SSFSE) or Half-fourier Single-shot Turbo spin-Echo (HASTE).[10] Since SSFSE acquires data in a single acquisition the TR is effectively infinitely long. Although acquiring data in as few a shots as possible sounds attractive from an acquisition time perspective, it should be realised that the underlying MRI signal decays during the acquisition period resulting in image blurring that increases with the ETL.[11]

Fig. 1 shows an example of negative colonography where the patients' colon has been rectally insufflated with CO_2, resulting in a dark luminal signal. In this case a proton density weighted SSFSE sequence has been used with a short effective TE. Fig. 2 shows an example of an SSFSE sequence used to obtain an image of the stomach and small bowel following oral water. Water not only increases the proton density but it also has a long T_2 relaxation time. This means that using a long effective TE can further enhance the contrast between the stomach and the surrounding tissues.

Although the vast majority of MRI involves imaging of protons (^{1}H) it is possible to image other NMR active nuclei that do not occur naturally in the body such as hyperpolarized nobel gases, e.g. helium (^{3}He) used for lung imaging.[12] Other NMR active nuclei such as hyperpolarized carbon (^{13}C),[13] and fluorine (^{19}F),[14] are currently being investigated in animal models. A major advantage of using these techniques is that the images are free of any background, i.e. proton density signals.

All these other nuclei require special methods of generating the agents and MRI system hardware capable of operating at the different Larmor frequencies. Whilst it is possible to acquire images of these nuclei using conventional MRI techniques retuned to the Larmor frequency of interest optimal imaging may require further pulse sequence modifications that are beyond the scope of this article.

Relaxation times

As discussed above the primary application of contrast *agents* is based upon their effect of reducing the T_1, T_2 and also the T_2* relaxation times of tissue water in the vicinity
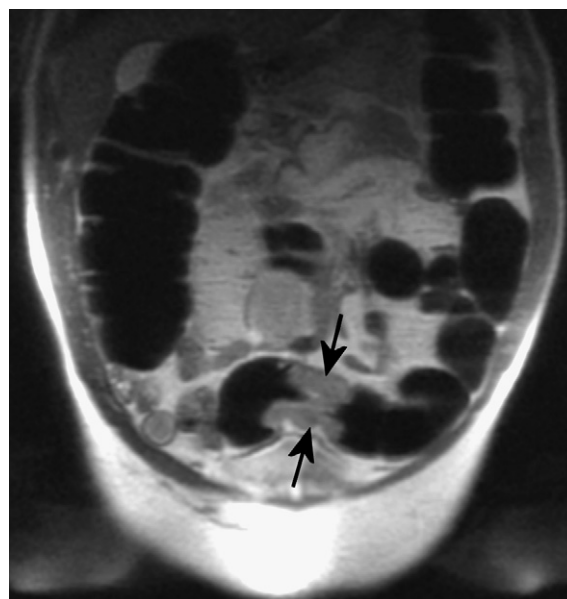

Figure 1 Proton density weighted single shot fast spin echo (SSFSE, GE Healthcare Technologies, Milwaukee) image of the colon following rectal administration of CO_2. Note the negative luminal signal. A carcinoma of the sigmoid colon is shown (arrows).

Figure 2 T_2-weighted single shot fast spin echo (SSFSE, GE Healthcare Technologies, Milwaukee) image of the stomach and small bowel following oral administration of water. Note the positive lumenal signal.

of the agent. How close the tissue water needs to approach the agent depends upon the relaxation mechanism. In the case of T_1 and T_2 relaxation water molecules need to approach the outer shell electrons of the paramagnetic or ferromagnetic species in order to experience the large electron magnetic moment that causes relaxation. This effect is therefore very short range. However, these species also cause a perturbation of the local magnetic field over a much larger spatial extent which means that T_2^* relaxation occurs over a much larger distance.[15] Note that T_2^* the effective transverse relaxation time is given by

$$\frac{1}{T_2^*} = \frac{1}{T_2} + \frac{1}{T_2'} \tag{2}$$

where T_2 is the natural decay and T_2' is the effect of magnetic field inhomogeneities. The agent will reduce both the T_2 and the T_2^* of the tissue with the primary effect being determined by the pulse sequence being used. Spin echo-based sequences will refocus the microscopic T_2' influences and the contrast will be primarily affected by the T_2 component, whereas gradient echo-based sequences will be influenced by both T_2 and T_2' effects, i.e. T_2^*.

Contrast agents do not exclusively affect only the T_1 or T_2 of the tissue but will affect both according to the relaxivity of the agent and its concentration. Following the administration of a paramagnetic compound the observed tissue relaxivity ($1/T_{1,2\ (observed)}$) becomes a linear combination of the intrinsic relaxivity ($1/T_{1,2\ (intrinsic)}$) of the tissue and the relaxivity of the agent ($1/T_{1,2\ (agent)}$).

$$\frac{1}{T_{1,2(observed)}} = \frac{1}{T_{1,2(intrinsic)}} + C\frac{1}{T_{1,2(agent)}} \tag{3}$$

where C is the concentration of the agent. It should be noted that since T_1 is generally an order of magnitude (10 times) longer than T_2 in most biological tissues there is a relatively larger reduction in T_1 for a given C in comparison to

T_2. For example using a gadolinium agent with a relaxivity of $3.4\ mM^{-1}s^{-1}$ and a concentration of 0.5 mM will cause a pre-contrast T_1 of 1000 ms to reduce to 370 ms, whereas the pre-contrast T_2 of 100 ms will only be reduced to 84 ms.

Using Eqs. (1) and (2), Fig. 3 shows the change in signal intensity for a hypothetical tissue with an intrinsic T_1 of 1000 ms and a T_2 of 100 ms as a function of contrast agent concentration for a T_1-weighted spin echo sequence with a TR of 500 ms and a TE of 10 ms and a T_2-weighted sequence with a TR of 5 s and a TE of 100 ms.

The graph shows that the addition of the agent decreases the T_1 relaxation time resulting in an increase in signal on T_1-weighting (positive contrast) and a decrease in signal on T_2-weighting (negative contrast). It should also be noted that as the concentration increases above approximately 2 mM, T_2 effects start to dominate and the signal intensity starts to decrease on T_1-weighting. This effect explains the phenomenon of pseudolayering of Gd-DTPA often noted in the urinary bladder.[16]

For gradient echo imaging the situation becomes a little more complex because we now have to take into consideration the excitation flip angle α. A simplified expression for an incoherent gradient echo sequence, e.g. SPGR (GE Healthcare Technologies), FLASH (Siemens Medical Solutions) or T_1-FFE (Philips Medical Systems), is given by

$$SI \propto \rho \frac{\sin\alpha\left(1 - e^{-\frac{TR}{T_1}}\right)e^{-\frac{TE}{T_2^*}}}{1 - \cos\alpha\, e^{-\frac{TR}{T_1}}} \tag{4}$$

Note that in the case of a gradient echo sequence we use T_2^* instead of T_2 since we are not using any refocusing pulses to eliminate the effects of the magnetic field inhomogeneities. If the TE is kept as short as possible to minimise T_2^* effects then this sequence is quite effective at producing T_1-weighted images.
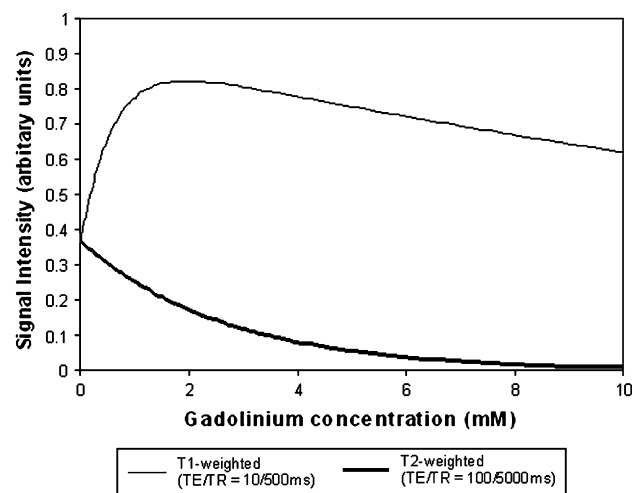

Figure 3 Graph showing the signal intensity changes with gadolinium concentration for a T_1-weighted (thin line) and T_2-weighted (thick line) standard spin echo pulse sequence. Note that the signal intensity decreases on the T_2-weighted image whereas the signal intensity initially increases on the T_1-weighted image until T_2 effects start to dominate and the signal intensity starts to decrease.

The expression for a coherent gradient echo sequence, e.g. FIESTA (GE Healthcare Technologies), True-FISP (Siemens Medical Solutions), balanced–FFE (Philips Medical Systems), is more complex but can be simplified for the case where the TR $\ll T_1, T_2$.

$$SI \propto \rho \frac{\sin\alpha}{1 + \cos\alpha + (1 - \cos\alpha)\left(\frac{T_1}{T_2}\right)} \qquad (5)$$

The evolution of the magnetisation in this sequence means that even though it is classed as a gradient echo sequence its contrast behaviour is dictated by the ratio of T_2/T_1 and T_2^* does not feature. This can be explained by the fact that the dephasing induced by the magnetic field inhomogeneities will be completely refocused at TE = TR/2 leading to the formation of a spin echo rather than a gradient echo.[17] In addition the TE and TR do not feature, only the flip angle, which means that this sequence can, and in fact should, be run with the shortest possible TE and TR and ideally balanced so that TR = 2*TE. The short acquisition time of this sequence means it has found applications in abdominal and cardiac imaging. However, since the administration of a contrast agent tends to make the ratio T_2/T_1 approach unity the images obtained do not benefit from the use of contrast agents.[18]

Contrast-enhanced morphological imaging

The majority of morphological contrast-enhanced imaging utilise conventional spin echo imaging sequences for T_1-weighted imaging and usually fast spin echo sequences for T_2-weighted imaging. The insensitivity to T_2^* effects makes the spin echo sequence ideally suited to post-contrast morphological imaging. One disadvantage of post-contrast T_1-weighted spin echo imaging is increased ghosting artefacts due to strong signal enhancement in moving structures or flowing blood, e.g. peristaltic ghosting artefacts in the bowel following administration of a positive oral contrast agent.[19] The ability to acquire fast spin echo images in a single breath-hold allows abdominal images to be acquired without respiratory artefacts which makes them the most suitable sequences for imaging negative contrast agents.[19]

Contrast-enhanced magnetic resonance angiography

The most common application for contrast-enhanced gradient echo imaging is in the technique of contrast-enhanced magnetic resonance angiography (CE-MRA).[20] In this application, volumetric (3D) data are acquired, using an incoherent (T_1-weighted) gradient echo sequence, during the first pass of a gadolinium-based paramagnetic contrast agent through the vascular anatomy of interest. The shortest possible TR is used to maximise the volumetric coverage in the shortest possible scan time, whilst the shortest possible TE, subject to SNR constraints, is used to minimise flow-related dephasing and also to minimise the effect of T_2^* signal loss due to the transiently high concentration of gadolinium. Sequences often employ fractional, or partial, echo acquisition in order to further reduce TE and consequently TR.[21] Once the volumetric slices have been acquired the data are usually displayed as a maximum intensity projection (MIP) where the brightest pixels along a line of sight through the volume are displayed in the final image.

When injecting gadolinium as a bolus there is a transient increase in the blood concentration [Gd] that results in a decrease in the observed T_1 of the blood from its intrinsic value of approximately 1200 ms. Fig. 4 shows the decrease in T_1 with increasing [Gd] together with the increasing signal intensity in a spoiled gradient echo sequence (SPGR) with a TE of 2 ms, a TR of 4 ms and a flip angle of 45°. A typical CE MRA study with an injection rate of 2 cc/s will reduce the T_1 of blood to around 25 ms. Fig. 5 shows MIPs of a 3D coronal acquisition through the thorax before and after bolus administration of Gd-DTPA. In the pre-image the blood flow is saturated due to the relatively long T_1 of blood, whereas in the post-image the vasculature is bright due to the considerably shortened T_1 of blood.

Whilst the underlying principle of contrast-enhanced MRA is the use of a T_1-weighted gradient echo imaging sequence there has been enormous technical developments in recent years directed at optimising the data acquisition with respect to the administration of the contrast agent. When injecting the agent as a bolus there is a short time window between the agent appearing in the arterial circulation but not reaching the venous circulation. This window is substantially shorter than a complete MRA acquisition so it is necessary to tailor the acquisition such that the centre of the MRI raw data matrix, or k-space, is acquired during this arterial window. In this way the bulk of the contrast in the angiogram represents the signal in the arterial vasculature uncontaminated by venous enhancement. The periphery of k-space, that provides the "detail" in the image, may then be acquired. Signal in the venous circulation during this time will have very little deleterious effect on the images. Therefore synchronising the acquisition with the peak first pass of the contrast agent requires knowledge of the delay, or circulation, time between the injection and the contrast reaching the area of interest and a means of acquiring the centre of k-space first.
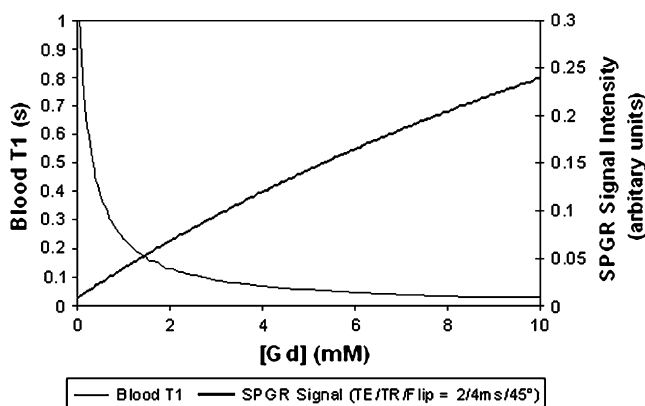

Figure 4 Graph showing the decrease in the T_1 of blood with increasing gadolinium concentration (thin line) together with the increase in signal intensity on 3D spoiled gradient echo (SPGR) sequence (thick line). A bolus injection rate of 2–3 cc/s is sufficient to produce a transient increase in the blood gadolinium concentration of approximately 10 mM.
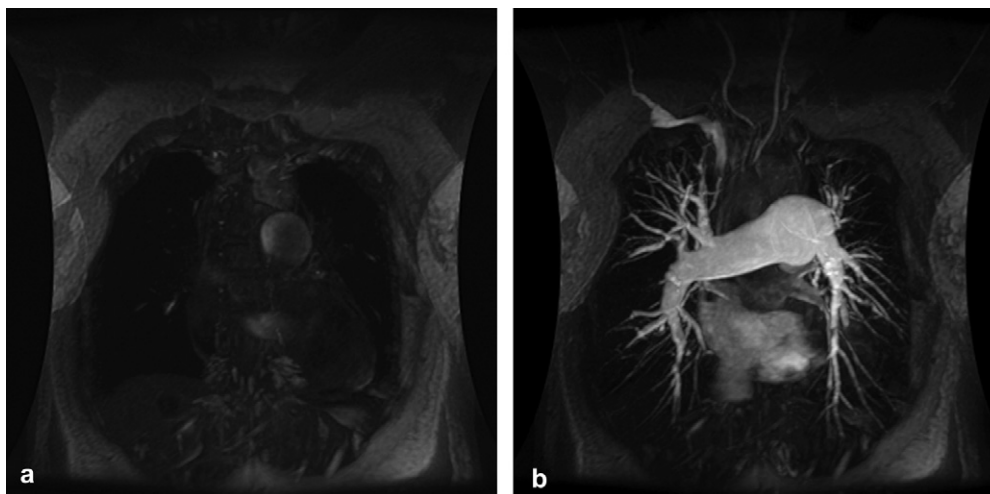
Figure 5 (a) Shows the maximum intensity projection (MIP) of a coronally acquired 3D volume prior to the administration of Gd-DTPA. Note that the unenhanced blood T_1 of approximately 1200 ms results in negligible signal. (b) Shows the MIP following the administration of 20 cm^3 of Gd-DTPA at 2 cc/s timed for the pulmonary arterial circulation.

The circulation time can be estimated for each patient individually or even standardized,[22] however, the best and most consistent results are obtained by optimising the timing, either retrospectively or prospectively.

The retrospective method involves the injection of a small test bolus, typically 2 ml, of contrast whilst rapidly and repeatedly imaging a slice through the vessel at the level of interest. Performing a region of interest analysis of the images shows a peak in the signal intensity at the time when the contrast reaches the area of interest. If imaging is started at the same time as the injection then this time is the circulation time.[23]

There are currently two prospective triggering methods. The first uses a rapid one-dimensional (1D) monitoring sequence that detects the increase in signal intensity as the contrast agent arrives in the area of interest (or lower in the arterial path) and starts the 3D MRA sequence automatically.[24,25] The second method uses rapid ''fluoroscopic'' imaging at the level of interest so that the operator can see the contrast arrive and then manually start the MRA sequence.[26] For both triggering methods the MR system also needs to provide a rapid switch over between the monitoring sequence and the actual 3D CE MRA sequence.

The true centre of 3D k-space is most effectively sampled using elliptic centric ordering[26] or one of its variants.[27,28] In a conventional encoded 3D sequence the entire slice-encoding (k_{SS}) loop is acquired before the k_{PE} phase encoding step is changed. So even if the phase encoding were centrically ordered (i.e. starting at zero and increasing to the maximum, alternating between positive and negative) we would be acquiring central k_{SS} lines right through the acquisition. The elliptic centric ordering acquires the k_{SS} and k_{PE} lines in a spiral fashion starting from the centre and moving outwards depending upon the actual spacing in k-space for each k_{PE} and k_{SS} step. In this way all the central k-space lines are acquired together. This ordering means that the centre of k-space is acquired almost a factor of 10 times faster than a conventional centric acquisition. Therefore scans with a much higher spatial resolution can be obtained even though the overall scan

time will be many times longer than the arterial-venous transit time.[29]

Recently parallel imaging techniques such as SENSE,[30] SMASH[31] and GRAPPA[32] have been developed that exploit multi-channel coil arrays to allow reductions in MR imaging times without sacrificing spatial resolution, albeit at a reduction in SNR. When applied in combination with elliptic centric acquisitions SENSE has been demonstrated to reduce venous contamination by 20%[33] and to produce higher SNR with reduced truncation artefacts at higher injection rates.[34]

In comparison to conventional angiography, CE-MRA is generally a static imaging technique and gives very little information on flow dynamics. There are a number of methods by which multiphase 2D single-slice projection[35,36] or 3D volume[37,38] CE-MRA acquisitions can be performed. A 3D volume could be repeated multiple times but the temporal resolution would be quite poor unless the time for an individual volume is reduced. The most common methods for reducing scan time in 3D CE MRA are to use the shortest possible TR, to use partial Fourier acquisitions and to decrease the resolution, particularly in the phase-encoding and slice-selection directions. The reduction in acquisition resolution can be partly offset through the use of zero-filling interpolation methods. If repeated fast enough then a pure arterial phase volume should occur in least at one of the acquisitions.[37] Alternatively only the central k-space data can be repeatedly acquired, a technique known as keyhole imaging. This has been demonstrated to acquire 3D volumes of the carotid at a rate of 3.6 per second.[38] As discussed above, parallel imaging techniques such as SENSE can also be employed to reduce the acquisition time for an individual volume.[39] Alternatively methods that leverage the relationship between the bulk of the image contrast and the acquisition of the centre of k-space can be used to acquire volumes at a greater temporal resolution. Time-resolved imaging of contrast kinetics (TRICKS) is one such method that segments k-space into a central volume and multiple concentric peripheral volumes.[40] During the TRICKS acquisition the volumes nearer

the centre of k-space are repeatedly acquired more rapidly than the outer volumes. Multiple volumes are then reconstructed with a higher temporal resolution than could be obtained by acquiring a complete 3D acquisition for each phase, although there will be some compromise in spatial resolution.[41] These dynamic techniques also obviate the need for operator triggering, potentially making them more robust.[42] Fig. 6 shows eight frames from a time-resolved TRICKS acquisition in the calf. Time-resolved techniques also permit the application of sophisticated post-processing techniques to improve the separation of arteries and veins.[43]

The use of standard extracellular gadolinium agents, e.g. Gd-DTPA has driven the technical development of pulse sequences for MRA. However, the recent commercialisation of a gadolinium-based blood-pool agent (Vasovist, Schering, Berlin) opens up the possibility of imaging in the equilibrium phase. Following injection this agent binds strongly to human serum albumin and remains intravascular for several hours, allowing the possibility of high-resolution T_1-weighted imaging to be performed in multiple planes. Whilst the agent can still be imaged during the first pass, potentially giving an improved CE MRA study since it has a considerably higher T_1 relaxivity than Gd-DTPA, in the equilibrium phase both arteries and veins enhance equally posing problems in separation.

Dynamic contrast-enhanced (DCE) MRI

Conventional contrast-enhanced imaging demonstrates the spatial uptake of a contrast agent, however, variations in microvascular structure and pathophysiology give rise to temporospatial variations in the enhancement of tissues that can provide valuable information for diagnosis and therapeutic follow-up. Dynamic contrast-enhanced (DCE) MRI acquires repeated images, at an appropriate rate, i.e. dynamically, during the passage of a contrast agent through the anatomy/pathology of interest. These images may then be subjected to simple visual analysis or more sophisticated mathematical analysis of the signal changes. Such analyses may range from basic semi-quantitative summary parameters such as the maximum slope of the signal changes through to quantitative pharmacokinetic modelling. Typical applications for DCE—MRI include myocardial ''perfusion'' and tumour imaging.

In terms of pulse sequences there are two major approaches to the acquisition of DCE—MRI data. Relaxivity-based methods use T_1-weighted acquisitions, whilst dynamic susceptibility contrast (DSC) techniques use T_2 or more commonly T_2^*-weighted acquisitions. DSC acquisitions are covered in more detail below. Acquisition of DCE images using relaxivity effects most commonly involves the use of a T_1-weighted gradient echo sequence in order to achieve an acceptable temporal resolution. Standard gradient echo sequences can provide a moderate degree of T_1-weighting, but pre-pulses such as saturation (90°) or inversion (180°) allow a significantly higher T_1-weighting to be achieved.[44] Fig. 7 shows six phases during the first pass of Gd-DTPA through the myocardium in the short axis plane. The increase in signal intensity can be seen as the contrast-enhanced blood passes through the right ventricle, then the left ventricle and finally into the myocardium. Note the lack of enhancement in the subendocardial region indicative of a perfusion defect.

Even using a gradient echo sequence it is still generally necessary to optimise the imaging parameters in order to achieve an appropriate trade-off between spatial and temporal resolution as well as coverage.[45] Various techniques have also been employed to try and reduce the
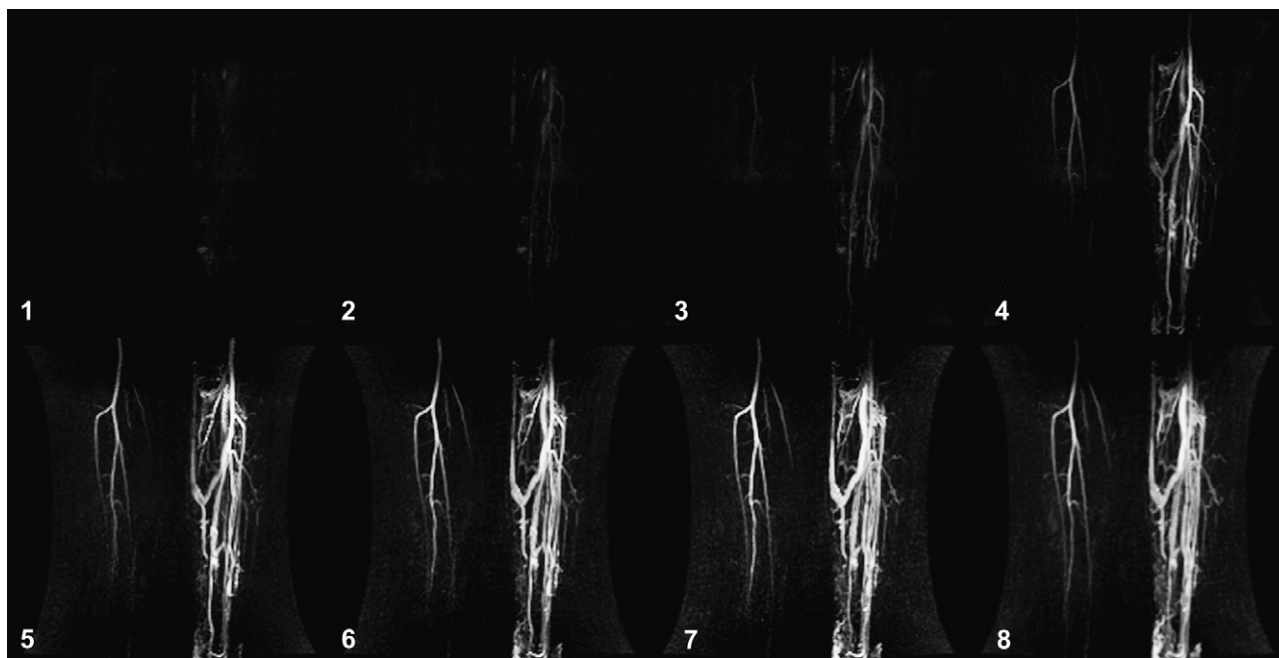
Figure 6 Eight frames from a time-resolved imaging of contrast kinetics (TRICKS) acquisition showing maximum intensity projections from each 3D volume in the calf. Note the differential flow patterns between the normal right leg and the arteriovenous malformation in the left leg.
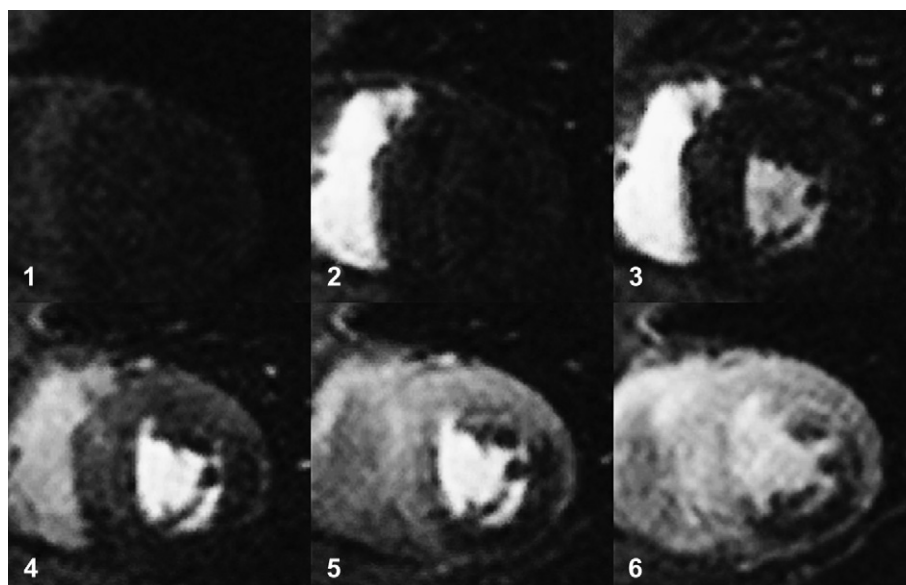
Figure 7   Six phases from a dynamic contrast-enhanced (DCE) study of myocardial perfusion using a saturation prepared fast gradient echo imaging sequence acquired in the cardiac short axis. The time interval between phases is two heartbeats. (1) Shows the myocardial signal suppression produced by the saturation pulse prior to the contrast agent arrival. (2) The contrast agent arrives in the right ventricle. Since this is a relaxivity effect and we are using a T_1-weighted acquisition the signal intensity increases. (3) The contrast agent starts to arrive in the left ventricle. (4) Strong enhancement in the left ventricle. (5) As the contrast agents flow through the myocardial capillaries there is signal enhancement in the myocardium, lack of signal enhancement in the subendocardial region reveals a perfusion defect that is shown more clearly in the next phase (6).

acquisition time, and thereby allow greater slice coverage for a given temporal resolution. Short echo-planar imaging (EPI) readouts have been employed, where a small number of echoes, typically four, are acquired after a single excitation pulse. Such short echo trains are used as a trade-off between reducing the acquisition time whilst minimising the artefacts that arise from extended echo trains.[46] Other approaches include the use of the ''keyhole'' imaging technique,[47] whereby only the central segment (keyhole) of a pre-contrast full *k*-space acquisition is updated for each temporal phase, i.e. the pre-contrast peripheral *k*-space segment is reused for each phase. Spatial parallel imaging techniques mentioned above can be used to reduce the acquisition time for each phase. In addition temporal acceleration techniques can also be used such as TSENSE,[48] UNFOLD[49] and k-t BLAST/k-t SENSE.[50]

Magnetic susceptibility

Magnetic susceptibility is the degree of magnetisation of a material in response to a magnetic field. Paramagnetic materials strengthen the magnetic field whereas diamagnetic materials weaken it. Gadolinium has seven unpaired electrons in its outer shell making it a paramagnetic metal ion. Therefore it has a large magnetic moment that causes a local spatial variation or inhomogeneity in the magnetic field. This spatial inhomogeneity causes the transverse relaxation of spins to be accelerated, resulting in the T_2^* signal decay described above. In many cases T_2^* relaxation is undesirable; indeed spin echo sequences were developed in part to ameliorate this effect. However, in those situations where this effect is desirable the sensitivity of

gradient echo-based imaging sequences to T_2^* relaxation means that they are well suited to visualising this particular property of a contrast agent. The most important imaging parameter for susceptibility imaging is the amount of phase dispersion caused by the combination of the pulse sequence parameters and the contrast agent. As the phase spread increases then signal cancellation starts to occur. The phase spread $\Delta\phi$ within a single voxel is given by the equation:

$$\Delta\phi \propto \Delta\chi\, \Delta r\, \mathrm{TE} \qquad (6)$$

where γ is the gyromagnetic ratio, Δr the voxel size, TE the echo time and $\Delta\chi$ is the difference in the local magnetic susceptibilities between the agent compartment and the surrounding tissue and is given by

$$\Delta\chi \propto 4\pi\chi_{\mathrm{m}}\, C \qquad (7)$$

where χ_{m} is the agent molar susceptibility and C is the agent concentration.

In terms of the pulse sequence it can therefore be seen that increasing either the pixel size, at the expense of spatial resolution, or increasing TE at the expense of overall image signal-to-noise ratio (SNR) can increase the amount of phase spread within a voxel.

Dynamic susceptibility contrast (DSC) MRI

One example of the advantageous effects of T_2^* relaxation is in dynamic susceptibility contrast (DSC) imaging using MRI. The approach is similar to the DCE technique described above but in this case we are using the susceptibility effect of the contrast agent rather than the relaxivity effect. For DSC imaging a bolus injection of the paramagnetic contrast agent is administered and dynamic, T_2^*-weighted imaging is

then used to monitor the first pass of the agent's passage through the organ of interest. T_2*-weighted imaging is often used in imaging blood flow within the brain because the contrast agent does not cross the intact blood—brain barrier and, since the capillary density is only 4%, there is a necessity to use an agent that causes a ''long-range'' effect in order to be detectable.[51] Fortunately techniques such as single shot echo-planar imaging (ssEPI) fulfil the two requirements of being sensitive to T_2* effects, by virtue of a long effective TE, and fast enough to track the transient passage of the contrast agent throughout the entire brain with sufficient temporal resolution.[52] Fig. 8 shows 12 images from a dynamic EPI acquisition before and during the first pass of a paramagnetic contrast agent through the brain. Note that during the first pass of the agent there is a marked decrease in the signal intensity within the brain parenchyma compared to the pre-image. This is due to the T_2* signal reduction caused by the magnetic field inhomogeneity that occurs as the agent passes through the capillaries. Note that despite the capillaries only occupying 4% of the brain tissue there is a marked signal reduction. These dynamic images can be analysed to produce parametric images that represent the spatial distribution of the cerebral blood volume and potentially cerebral blood flow.[53]

(Ultra)-small paramagnetic iron oxide ((U)SPIO) imaging

Another application of T_2*-weighted imaging is following the administration of SPIO or USPIO agents. In this situation accumulation of the particles causes a decrease in signal intensity due to susceptibility-induced relaxation. The majority of studies that have used USPIO particles have used long TE (10—20 ms) gradient echo sequences; however, it should also be noted that USPIO particles of less than 10 nm in size also cause a large reduction in T_1. Indeed some USPIO agents are developed as blood-pool agents for magnetic resonance angiography.[54,55] Therefore depending upon the concentration and biodistribution of the agent it may have a confounding T_1 signal enhancing effect in addition to the signal decay due to T_2* resulting in the presence of the agent being obscured.[56] Therefore the optimal visualisation of the agent should involve the use of a gradient echo sequence where the effects of T_1 can be minimised
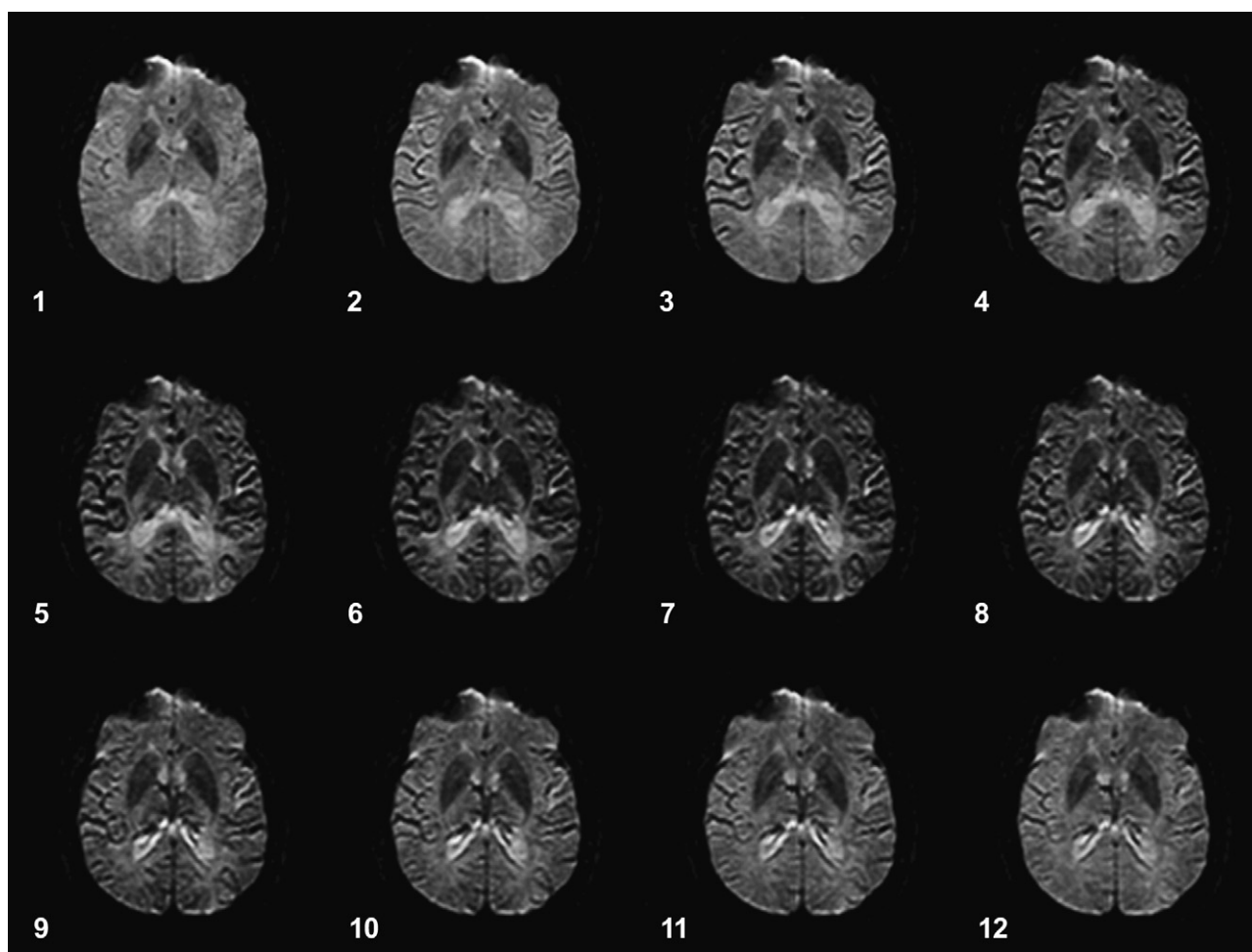

Figure 8   Twelve phases from a dynamic susceptibility contrast (DSC) study in the brain using an echo planar imaging sequence (EPI). The time between images is 1 s. Note that as the Gd-DTPA contrast agent bolus passes through the cerebral circulation there is a strong, but transient, signal intensity decreases due to the T_2* dephasing caused by the agent.

by, for example, the use of a long TR and low flip angle. The optimal choice of echo time is also difficult to determine a priori since too short a TE may not allow sufficient susceptibility-induced phase spread and hence signal loss whilst too long a TE may result in unnecessary sacrificing of image signal to-noise ratio (SNR). Multi-echo gradient echo sequences are very useful in these applications since they allow multiple images acquisitions at different echo times. The individual echoes can be visually inspected to illustrate the change in signal intensity or, if the appropriate software is available, they can be used to calculate the T_2^* relaxation time on a pixel-by-pixel basis.[56]

Resonant frequency shift

In addition to the bulk magnetic susceptibility effect caused by a paramagnetic agent it is also possible for the agent to shift the local proton resonant frequency. If we mathematically model the compartment as an infinitely long cylinder, i.e. like a blood vessel at an angle θ to the static magnetic field B_0 then it can be shown that the frequency shift, $\delta\nu$, is given by

$$\delta\nu = \frac{\gamma B_0}{4\pi} \Delta\chi \left(\cos^2\theta - \frac{1}{3}\right) \tag{8}$$

Whilst metal ions like gadolinium are efficient relaxivity agents as well as susceptibility agents, ions such as dysprosium (Dy^{3+}) are mainly efficient susceptibility agents. Indeed a Dy^{3+}-based contrast agent has been used as an improved T_2^* perfusion agent although toxicity issues have limited its application to a phase I clinical trial.[57]

A major disadvantage of the use of SPIO agents is that the bulk magnetic susceptibility effect results in regions of hypointensity or negative contrast on T_2- or T_2^*-weighted imaging that can be difficult to separate from naturally occurring voids in the image. Recently there has been interest in the imaging of the frequency shift caused by the dipolar field that surrounds the particles as a positive contrast or ''white marker'' effect, particularly for the imaging of stem cells labelled with SPIO particles.[58,59] The basic principle behind the technique is that SPIO particles generate a highly localised and non-linear magnetic field that normally has the effect of dephasing the local signal resulting in the signal void. White marker techniques attempt to acquire the signal within a small range of the SPIO-induced frequency shifts. Since this frequency shift is different from the normal proton frequency the SPIO particles appear as a signal hyperintensity against a dark background. Fig. 9 shows two images of a gelatine phantom containing USPIO particles (Sinerem, Guerbet, Paris): (a) shows the conventional T_2 signal loss whilst; (b) shows the positive signal obtained using an implementation of the sequence described by Stuber et al.[58] Whilst there are a number of approaches to imaging this positive signal a simple implementation uses a gradient echo sequence in which the slice selection gradient is deliberately left unrefocused causing a general loss of signal in the image.[60] Since the SPIO particles cause a spatially distributed magnetic field shift at one region in this field the combination of the rephasing gradient and the SPIO-induced magnetic field will match the slice select gradient resulting in a perfect refocusing and
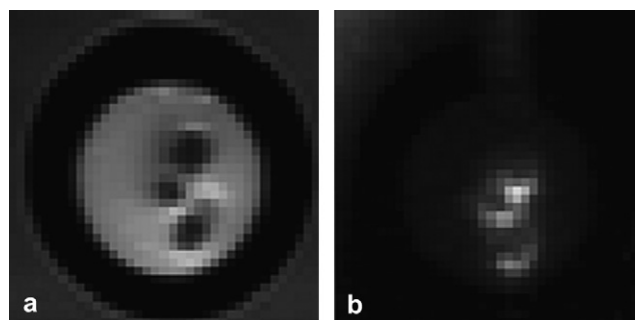

Figure 9 (a) Shows a gelatin phantom in which ultrasmall paramagnetic iron oxide (USPIO) particles (Sinerem, Guerbet, Paris) have been injected. The T_2 effect causes a loss of signal. (b) The same phantom is imaged using an off-resonance imaging technique[58] that shows the effect of the particles as a positive signal.

a positive signal. Although USPIO labelled stem cell experiments are still only being performed in animal models these positive contrast techniques show considerable promise for stem cell trafficking studies.

Summary

This review has outlined some of the pulse sequence approaches that have been used to image tissue following the administration of contrast agents. The primary application remains morphological imaging following the administration of either a positive or a negative relaxivity-based agent. Magnetic resonance angiography is probably the next biggest application requiring rapid image acquisition during the first pass of a positive relaxivity-based agent. Dynamic contrast-enhanced imaging is a rapidly developing field that allows the contrast agent kinetics to be measured, potentially providing quantitative information on organ or tumour function. Finally the combination of novel MRI pulse sequences together with the recent developments in targeted contrast agents discussed in the paper by Yan and Hogg in this issue offers the potential for practical cellular and molecular imaging by MRI.

References

1. Bloch F, Hansen WW, Packard M. The nuclear induction experiment. *Phys Rev* 1946;**70**:474—85.
2. Weinmann HJ, Brasch RC, Press WR, Wesbey GE. Characteristics of gadolinium-DTPA complex: a potential NMR contrast agent. *AJR Am J Roentgenol* 1984;**142**:619—24.
3. Carr DH, Brown J, Bydder GM, Steiner RE, Weinmann HJ, Speck U, et al. Gadolinium-DTPA as a contrast agent in MRI: initial clinical experience in 20 patients. *AJR Am J Roentgenol* 1984;**143**:215—24.
4. McRobbie DW, Moore EA, Graves MJ, Prince MR. *MRI: from picture to proton.* Cambridge: Cambridge University Press; 2003.
5. Lomas DJ, Habib SH, Joubert IJ, Sala E, Graves MJ. CO_2 as a distending medium for gastric and small bowel MRI: a feasibility study. *Eur Radiol* 2005;**15**:672—6.
6. Lomas DJ, Graves MJ. Small bowel MRI using water as a contrast medium. *Br J Radiol* 1999;**72**:994—7.
7. Sood RR, Joubert I, Franklin H, Doyle T, Lomas DJ. Small bowel MRI: comparison of a polyethylene glycol preparation and

water as oral contrast media. *J Magn Reson Imaging* 2002;**15**: 401—8.

8. Umschaden HW, Szolar D, Gasser J, Umschaden M, Haselbach H. Small-bowel disease: comparison of MR enteroclysis images with conventional enteroclysis and surgical findings. *Radiology* 2000;**215**:717—25.

9. Hennig J, Nauerth A, Friedburg H. RARE imaging: a fast imaging method for clinical MR. *Magn Reson Med* 1986;**3**:823—33.

10. Semelka RC, Kelekis NL, Thomasson D, Brown MA, Laub GA. HASTE MR imaging: description of technique and preliminary results in the abdomen. *J Magn Reson Imaging* 1996;**6**:698—9.

11. Constable RT, Anderson AW, Zhong J, Gore JC. Factors influencing contrast in fast spin-echo MR imaging. *Magn Reson Imaging* 1992;**10**:497—511.

12. Middleton H, Black RD, Saam B, Cates GD, Cofer GP, Guenther R, et al. MR imaging with hyperpolarized ^{3}He gas. *Magn Reson Med* 1995;**33**:271—5.

13. Mansson S, Johansson E, Magnusson P, Chai CM, Hansson G, Petersson JS, et al. ^{13}C imaging-a new diagnostic platform. *Eur Radiol* 2006;**16**:57—67.

14. Schwarz R, Schuurmans M, Seelig J, Kunnecke B. ^{19}F-MRI of perfluorononane as a novel contrast modality for gastrointestinal imaging. *Magn Reson Med* 1999;**41**:80—6.

15. Fisel CR, Ackerman JL, Buxton RB, Garrido L, Belliveau JW, Rosen BR, et al. MR contrast due to microscopically heterogeneous magnetic susceptibility: numerical simulations and applications to cerebral physiology. *Magn Reson Med* 1991;**17**: 336—47.

16. Elster AD, Sobol WT, Hinson WH. Pseudolayering of Gd-DTPA in the urinary bladder. *Radiology* 1990;**174**:379—81.

17. Scheffler K, Hennig J. Is TrueFISP a gradient-echo or a spin-echo sequence? *Magn Reson Med* 2003;**49**:395—7.

18. Scheffler K, Lehnhardt S. Principles and applications of balanced SSFP techniques. *Eur Radiol* 2003;**13**:2409—18.

19. Grubnic S, Padhani AR, Revell PB, Husband JE. Comparative efficacy of and sequence choice for two oral contrast agents used during MR imaging. *AJR Am J Roentgenol* 1999;**173**:173—8.

20. Prince MR. Gadolinium-enhanced MR aortography. *Radiology* 1994;**191**:155—64.

21. Schmalbrock P, Yuan C, Chakeres DW, Kohli J, Pelc NJ. Volume MR angiography: methods to achieve very short echo times. *Radiology* 1990;**175**:861—5.

22. Levy RA, Prince MR. Arterial-phase three-dimensional contrast-enhanced MR angiography of the carotid arteries. *AJR Am J Roentgenol* 1996;**167**:211—5.

23. Kim JK, Farb RI, Wright GA. Test bolus examination in the carotid artery at dynamic gadolinium-enhanced MR angiography. *Radiology* 1998;**206**:283—9.

24. Foo TK, Saranathan M, Prince MR, Chenevert TL. Automated detection of bolus arrival and initiation of data acquisition in fast, three-dimensional, gadolinium-enhanced MR angiography. *Radiology* 1997;**203**:275—80.

25. Isoda H, Takehara Y, Isogai S, Takeda H, Kaneko M, Nozaki A, et al. Technique for arterial-phase contrast-enhanced three-dimensional MR angiography of the carotid and vertebral arteries. *AJNR Am J Neuroradiol* 1998;**19**:1241—4.

26. Wilman AH, Riederer SJ, Huston III J, Wald JT, Debbins JP. Arterial phase carotid and vertebral artery imaging in 3D contrast-enhanced MR angiography by combining fluoroscopic triggering with an elliptical centric acquisition order. *Magn Reson Med* 1998;**40**:24—35.

27. Willinek WA, Gieseke J, Conrad R, Strunk H, Hoogeveen R, von Falkenhausen M, et al. Randomly segmented central k-space ordering in high-spatial-resolution contrast-enhanced MR angiography of the supraaortic arteries: initial experience. *Radiology* 2002;**225**:583—8.

28. Watts R, Wang Y, Redd B, Winchester PA, Kent KC, Bush HL, et al. Recessed elliptical-centric view-ordering for contrast-enhanced 3D MR angiography of the carotid arteries. *Magn Reson Med* 2002;**48**:419—24.

29. Fain SB, Riederer SJ, Bernstein MA, Huston III J. Theoretical limits of spatial resolution in elliptical-centric contrast-enhanced 3D-MRA. *Magn Reson Med* 1999;**42**:1106—16.

30. Pruessmann KP, Weiger M, Scheidegger MB, Boesiger P. SENSE: sensitivity encoding for fast MRI. *Magn Reson Med* 1999;**42**: 952—62.

31. Sodickson DK, Manning WJ. Simultaneous acquisition of spatial harmonics (SMASH): fast imaging with radiofrequency coil arrays. *Magn Reson Med* 1997;**38**:591—603.

32. Griswold MA, Jakob PM, Heidemann RM, Nittka M, Jellus V, Wang J, et al. Generalized autocalibrating partially parallel acquisitions (GRAPPA). *Magn Reson Med* 2002;**47**:1202—10.

33. Hu HH, Madhuranthakam AJ, Kruger DG, Huston III J, Riederer SJ. Improved venous suppression and spatial resolution with SENSE in elliptical centric 3D contrast-enhanced MR angiography. *Magn Reson Med* 2004;**52**:761—5.

34. Riedy G, Golay X, Melhem ER. Three-dimensional isotropic contrast-enhanced MR angiography of the carotid artery using sensitivity-encoding and random elliptic centric k-space filling: technique optimization. *Neuroradiology* 2005;**47**:668—73.

35. Wang Y, Johnston DL, Breen JF, Huston III J, Jack CR, Julsrud PR, et al. Dynamic MR digital subtraction angiography using contrast enhancement, fast data acquisition, and complex subtraction. *Magn Reson Med* 1996;**36**:551—6.

36. Hennig J, Scheffler K, Laubenberger J, Strecker R. Time-resolved projection angiography after bolus injection of contrast agent. *Magn Reson Med* 1997;**37**:341—5.

37. Levy RA, Maki JH. Three-dimensional contrast-enhanced MR angiography of the extracranial carotid arteries: two techniques. *AJNR Am J Neuroradiol* 1998;**19**:688—90.

38. Melhem ER, Caruthers SD, Faddoul SG, Tello R, Jara H. Use of three-dimensional MR angiography for tracking a contrast bolus in the carotid artery. *AJNR Am J Neuroradiol* 1999;**20**:263—6.

39. Golay X, Brown SJ, Itoh R, Melhem ER. Time-resolved contrast-enhanced carotid MR angiography using sensitivity encoding (SENSE). *AJNR Am J Neuroradiol* 2001;**22**:1615—9.

40. Korosec FR, Frayne R, Grist TM, Mistretta CA. Time-resolved contrast-enhanced 3D MR angiography. *Magn Reson Med* 1996;**36**:345—51.

41. Fellner C, Lang W, Janka R, Wutke R, Bautz W, Fellner FA. Magnetic resonance angiography of the carotid arteries using three different techniques: accuracy compared with intraarterial x-ray angiography and endarterectomy specimens. *J Magn Reson Imaging* 2005;**21**:424—31.

42. Naganawa S, Koshikawa T, Fukatsu H, Sakurai Y, Ichinose N, Ishiguchi T, et al. Contrast-enhanced MR angiography of the carotid artery using 3D time-resolved imaging of contrast kinetics: comparison with real-time fluoroscopic triggered 3D-elliptical centric view ordering. *Radiat Med* 2001;**19**:185—92.

43. Korosec FR, Turski PA, Carroll TJ, Mistretta CA, Grist TM. Contrast-enhanced MR angiography of the carotid bifurcation. *J Magn Reson Imaging* 1999;**10**:317—25.

44. Haase A. Snapshot FLASH MRI. Applications to T_1, T_2, and chemical-shift imaging. *Magn Reson Med* 1990;**13**:77—89.

45. Krishnan S, Chenevert TL. Spatio-temporal bandwidth-based acquisition for dynamic contrast-enhanced magnetic resonance imaging. *J Magn Reson Imaging* 2004;**20**:129—37.

46. Ding S, Wolff SD, Epstein FH. Improved coverage in dynamic contrast-enhanced cardiac MRI using interleaved gradient-echo EPI. *Magn Reson Med* 1998;**39**:514—9.

47. Oesterle C, Strohschein R, Kohler M, Schnell M, Hennig J. Benefits and pitfalls of keyhole imaging, especially in first-pass perfusion studies. *J Magn Reson Imaging* 2000;**11**:312—23.

48. Kellman P, Epstein FH, McVeigh ER. Adaptive sensitivity encoding incorporating temporal filtering (TSENSE). *Magn Reson Med* 2001;**45**:846—52.

49. Madore B, Glover GH, Pelc NJ. Unaliasing by fourier-encoding the overlaps using the temporal dimension (UNFOLD), applied to cardiac imaging and fMRI. *Magn Reson Med* 1999;**42**:813—28.

50. Tsao J, Boesiger P, Pruessmann KP. k-t BLAST and k-t SENSE: dynamic MRI with high frame rate exploiting spatiotemporal correlations. *Magn Reson Med* 2003;**50**:1031—42.

51. Edelman RR, Mattle HP, Atkinson DJ, Hill T, Finn JP, Mayman C, et al. Cerebral blood flow: assessment with dynamic contrast-enhanced T_2*-weighted MR imaging at 1.5 T. *Radiology* 1990; **176**:211—20.

52. Cohen MS, Weisskoff RM. Ultra-fast imaging. *Magn Reson Imaging* 1991;**9**:1—37.

53. Rosen BR, Belliveau JW, Buchbinder BR, McKinstry RC, Porkka LM, Kennedy DN, et al. Contrast agents and cerebral hemodynamics. *Magn Reson Med* 1991;**19**:285—92.

54. Kellar KE, Fujii DK, Gunther WH, Briley-Saebo K, Bjornerud A, Spiller M, et al. NC100150 Injection, a preparation of optimized iron oxide nanoparticles for positive-contrast MR angiography. *J Magn Reson Imaging* 2000;**11**:488—94.

55. Li W, Tutton S, Vu AT, Pierchala L, Li BS, Lewis JM, et al. First-pass contrast-enhanced magnetic resonance angiography in humans using ferumoxytol, a novel ultrasmall superparamagnetic iron oxide (USPIO)-based blood pool agent. *J Magn Reson Imaging* 2005;**21**:46—52.

56. Harisinghani MG, Dixon WT, Saksena MA, Brachtel E, Blezek DJ, Dhawale PJ, et al. MR lymphangiography: imaging strategies to optimize the imaging of lymph nodes with ferumoxtran-10. *Radiographics* 2004;**24**:867—78.

57. Roberts TP, Kucharczyk J, Cox I, Moseley ME, Prayer L, Dillon W, et al. Sprodiamide-injection-enhanced magnetic resonance imaging of cerebral perfusion. Phase I clinical trial results. *Invest Radiol* 1994;**29**(Suppl. 2):S24—6.

58. Stuber M, Gilson WD, Schaer M, Bulte JW, Kraitchman DL. Shedding light on the dark spot with IRON — a method that generates positive contrast in the presence of superparamagnetic nanoparticles. *Proc Intl Soc Mag Reson Med* 2005;**13**:2608.

59. Cunningham CH, Arai T, Yang PC, McConnell MV, Pauly JM, Conolly SM. Positive contrast magnetic resonance imaging of cells labeled with magnetic nanoparticles. *Magn Reson Med* 2005;**53**:999—1005.

60. Mani V, Briley-Saebo KC, Itskovich VV, Samber DD, Fayad ZA. Gradient echo acquisition for superparamagnetic particles with positive contrast (GRASP): sequence characterization in membrane and glass superparamagnetic iron oxide phantoms at 1.5 T and 3 T. *Magn Reson Med* 2006;**55**:126—35.